J Mater Sci (2009) 44:2055–2062
DOI 10.1007/s10853-009-3304-3

Dispersion assessment and studies on AC percolative conductivity in polymer-derived Si–C–N/CNT ceramic nanocomposites

E. Ionescu · A. Francis · R. Riedel

Received: 23 September 2008 / Accepted: 28 January 2009 / Published online: 26 February 2009

Abstract Nanocomposites comprise polysilazane-derived SiCN ceramic charged with carbon nanotubes (CNTs) have been prepared by dispersion of multi-walled CNTs with a diameter of 80 nm in a cross-linked polysilazane (HTT 1800, Clariant) using a simple roll-mixer method. Subsequently, the composites were warm pressed and pyrolyzed in argon atmosphere. Scanning electron microscopy (SEM) and 3D Raman imaging techniques were used as major tools to assess the dispersion of CNTs throughout the ceramic matrix. Furthermore, studies on the effect of the volume fraction of CNTs in the nanocomposites on their electrical properties have been performed. The specific bulk conductivities of the materials were analyzed by AC impedance spectroscopy, revealing percolation thresholds (ρ_c) at CNT loadings lower than 1 vol%. Maximum conductivity amounted to 7.6×10^{-2} S/cm was observed at 5 vol% CNT. The conductivity exponent in the SiCN/CNT composites was found equal to 1.71, indicating transport in three dimensions.

Introduction

Carbon nanotubes (CNTs) are known as one-dimensional carbon materials with excellent properties, such as high Young's moduli [1–4], high tensile strength [5, 6], or axial thermal conductivity higher than that of diamond [7]. Furthermore, CNTs can show semiconducting or metallic behavior, depending on their diameters and chiralities [8–10]. The incorporation of CNTs in ceramics has attracted a great interest in the last years. Nevertheless, the preparation of ceramic–matrix CNT composites is limited due to the strong aggregation of the nanotubes in the matrix [11, 12]. Thus, carbon nanotubes are prone to form bundles due to van der Waals interactions, and therefore their dispersion is the limiting step in the preparation of nanocomposites. Furthermore, appropriate interfacial bonding between the CNTs and the matrix is an important condition to achieve for instance an improvement of mechanical properties.

Ceramic–matrix CNT composites are usually prepared by conventional powder technologies and high-temperature sintering processes. The disadvantage of these techniques rely on the fact that during processing the integrity of the CNTs is altered, thus the improvement of mechanical or electrical properties of the composites cannot be fulfilled. In the last years, some reports on an alternative preparation, namely polymer-derived ceramic (PDC) matrix CNT composites have been published [13–15]. The advantage of these materials consists of the possibility to incorporate the CNTs into a liquid preceramic polymer, which can increase the effectiveness of their dispersion. Nevertheless, the addition of the CNTs into the liquid precursor has to be done under ultrasonication condition, which may affect also their integrity.

In this paper we present the preparation of SiCN ceramic–matrix CNT composites by performing the incorporation of multi-walled CNTs into a solid cross-linked polysilazane using a mild role-mixing method.

Whereas published studies on polymer-derived ceramic–matrix CNT composites rather focus on their mechanical properties, our investigations were concentrated on the

E. Ionescu (✉) · R. Riedel
Technische Universität Darmstadt, Institute for Materials Science, Petersenstrasse 23, 64287 Darmstadt, Germany
e-mail: ionescu@materials.tu-darmstadt.de

A. Francis
Central Metallurgical Research and Development Institute (CMRDI), P.O. Box 87, Helwan, Cairo, Egypt

effect of the CNTs on the electrical properties of the nanocomposites, since to the best of our knowledge this feature has not been addressed yet for polymer-derived ceramic–matrix CNT composites.

Experimental

For the preparation of the SiCN/CNT composites a commercially available polysilazane (HTT1800, Clariant, Germany) was used. The polymer was manipulated and stored in a glove box (MBraun, Germany) under argon atmosphere of 99.999% purity. The polysilazane was filled into a quartz tube and cross-linked at 280 °C for 5 h in a vertical furnace with SiC heating elements (Fa. GERO, Germany). Subsequently, the cross-linked precursor was milled in a planet ball mill (30 min at 180 rpm) using zirconia milling balls, and sieved through a 32 μm sieve. Multi-walled CNTs (MER company, USA, purity > 95%, 80 nm diameter, 4 μm length) and the cross-linked polysilazane were mixed in different ratios using a roll-mixer (48 h at 90 rpm). Silicon nitride milling balls with diameter of 1.4 and 12 mm (ratio 1 to 2) were used for mixing at a ball power ratio (BPR) of 30. The homogenized mixtures were subsequently warm pressed at 200 °C (500 MPa, 60 min) and pyrolyzed at 1,100 °C and 1,300 °C, respectively, in argon atmosphere to obtain SiCN/CNT ceramic composites.

Scanning electron microscopy (SEM) investigations were performed using a Philips XL30 FEG microscope. Raman spectra (from 50 to 4,000 cm^{-1}) were recorded with a micro-Raman HR800 spectrometer (Horiba Jobin Yvon, Germany) using laser wavelength of 488 nm. *D* and *G* band positions as well as their full widths at half-height (FWHH) were determined by fitting the curves using Lorentzian and/or Gaussian routines.

Raman maps on sample surfaces (60 × 60 μm^2) of the composites containing different volume fractions of CNTs have been recorded in 1 μm steps in the region from 1,450 to 1,650 cm^{-1}. Thus, the uniformity of CNT dispersions throughout the ceramic matrix has been studied by mapping the change of the intensity of *G* band within the sample surface. This has been performed by using a 50× microscope objective to focus the laser beam (488 nm) on the sample surface.

AC impedance measurements were performed with a Precision LCR meter 4284A (Hewlet Packard) impedance spectrometer over a frequency range from 20 Hz to 1 MHz. The specific conductivity (σ) for the investigated samples was calculated as $\sigma = h/(R \cdot S)$, where S is the surface area of the sample, h is the sample thickness and R is the impedance measured experimentally.

Results and discussion

In this study Si–C–N ceramic–matrix CNT nanocomposites have been prepared and investigated with respect to CNT dispersion within the ceramic matrix. SEM investigations on the fracture surface of the monolithic SiCN/CNT composites pyrolyzed at 1,100 °C showed that the distribution of the carbon nanotubes throughout the matrix in the composite depends on the volume fraction of the CNTs loaded. Whereas the composite with 1 vol% CNTs showed a fair distribution, a uniform distribution of the CNTs was observed in composites with higher CNT volume fractions (Fig. 1). Furthermore, the SEM studies showed that the integrity and thus the aspect ratio of the CNTs were not altered during processing or pyrolysis.

Powder X-ray diffraction investigations showed that the matrix of the composites pyrolyzed at both temperatures, i.e., 1,100 and 1,300 °C, is amorphous. Thus, only one reflex for graphite ($2\Theta = 26.2$) was observed due to the presence of CNTs in the composites.

The SiCN/CNT composites were investigated via Raman spectroscopy in order to obtain information about the composition thereof and furthermore in order to assess the dispersion of the CNTs throughout the PDC matrix. Raman spectroscopy is a non-destructive method for characterizing carbon-containing materials like graphite [16], carbon

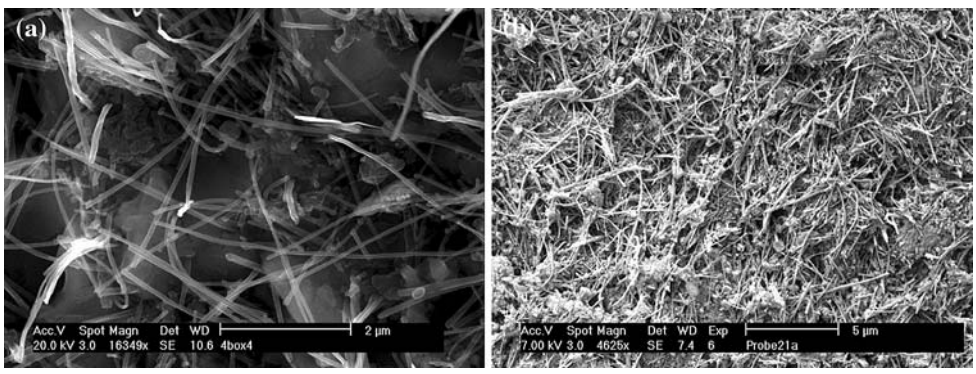

Fig. 1 Scanning electron microscopy (SEM) images of the fracture surface of SiCN/CNT composites containing 1 vol% (**a**) resp. 10 vol% (**b**) CNTs pyrolyzed at 1,100 °C

black-based materials [17, 18], amorphous carbon films [19], or carbon nanotubes and their composites [20–22]. The Raman spectrum of the as received carbon nanotubes used for the preparation of the composites (Fig. 2) shows beside two bands at 1,561.1 cm^{-1} (*G* band) and at 2,691.6 cm^{-1} (*G′* band) the spectrum presents a weak band at 1,344.4 cm^{-1} (*D* band), corresponding to the presence of amorphous carbonaceous products, disordered carbon [18] or defects in curved graphene sheets, tube ends and surviving impurities [23]. The band at 1,561 cm^{-1} is the Raman active *G*-band (E2g) originating from the in plane vibrational mode. The frequency downshift (21 cm^{-1}) of this band with respect to the *G*-band observed in natural single crystal graphite (1,582 cm^{-1}), is attributed to the curved and closed graphitic structures in nanotubes [24].

The Raman spectra of the SiCN/CNT nanocomposites pyrolyzed at 1,100 °C revealed the presence of both disorder-induced (*D*) and graphite-like (*G*) bands (Fig. 3). However, an influence of the CNT content on the position of the *D* and *G* bands as well as on their half-widths (FWHH) and on their intensity ratios has been observed (Table 1). This finding can be attributed to CNT–matrix interactions or more probably to the in situ generation of "free carbon" during the pyrolysis of the polysilazane matrix material, which is known to occur at temperatures above 1,000 °C [25].

The shift in the Raman bands position can be furthermore attributed to the shrinkage of the SiCN matrix which induces mechanical stresses in the incorporated CNTs [26, 27]. Thus, the carbon nanotubes experience a compressive deformation, as can be observed from the shift of ω_G from 1,561 cm^{-1} in the as received CNTs toward higher wave numbers in the SiCN/CNT composites. The half-widths (FWHH) of the *G* (504.3–114.7 cm^{-1}) and *D* bands (330.0–272.5 cm^{-1}) decrease with increasing content of CNTs in the composites pyrolyzed at 1,100 °C. In the case of the SiCN/CNT materials pyrolyzed at 1,300 °C the FWHH of the *G* band increases (86.8–252.7 cm^{-1}) while that of the *D* band (440.2–169.0 cm^{-1}) decreases with increasing CNT loading. The graphitization grade G_G (i.e., $I_G/(I_G + I_D)$) increases from 45.2% in SiCN to 54−57% by adding CNTs into the PDC matrix and seems also to be enhanced by increasing the pyrolysis temperature from 1,100 to 1,300 °C, which is however, much lower than G_G in the as received CNTs (92.4%). In the case of the SiCN/CNT sample containing 10 vol% CNTs the opposite trend has been observed, thus G_G was found to be lower than in the composites with lower CNT volume fraction loadings. This observation could unfortunately not be explained. Further systematic investigations on the influence of CNT content and of temperature on the G_G in the SiCN/CNT composites have to be performed.

The uniformity of CNTs dispersion throughout the SiCN matrix was studied furthermore by performing confocal Raman mapping of 60 × 60 μm^2 sample surfaces of the SiCN/CNT composites in the region of 1,450–1,650 cm^{-1}

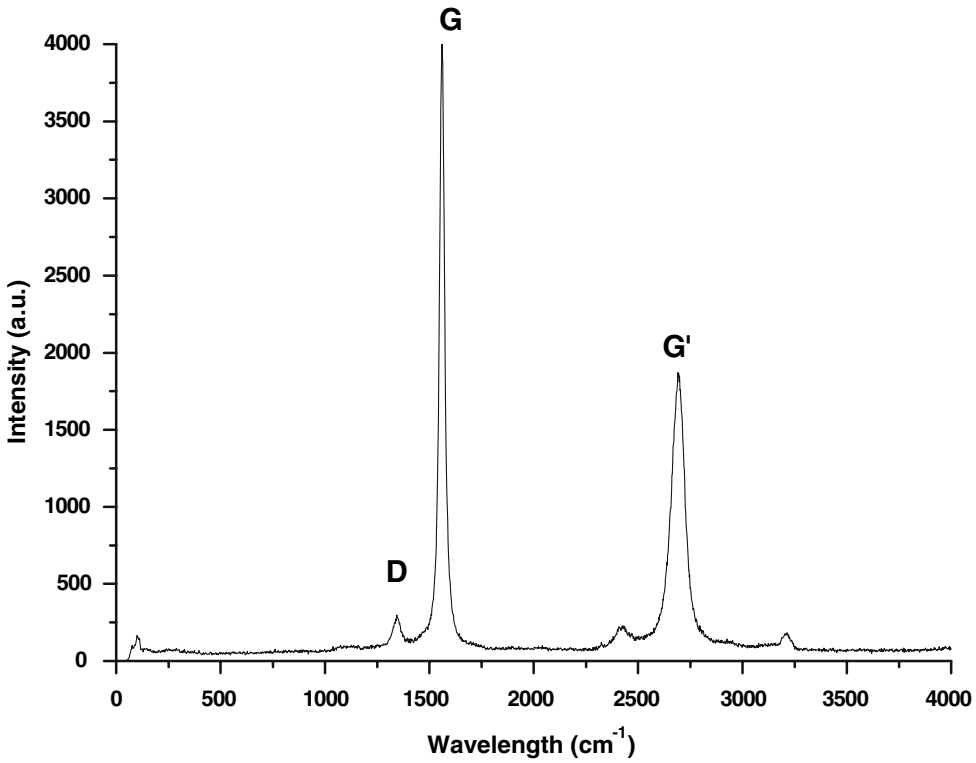

Fig. 2 Raman spectrum of as received multi-walled carbon nanotubes

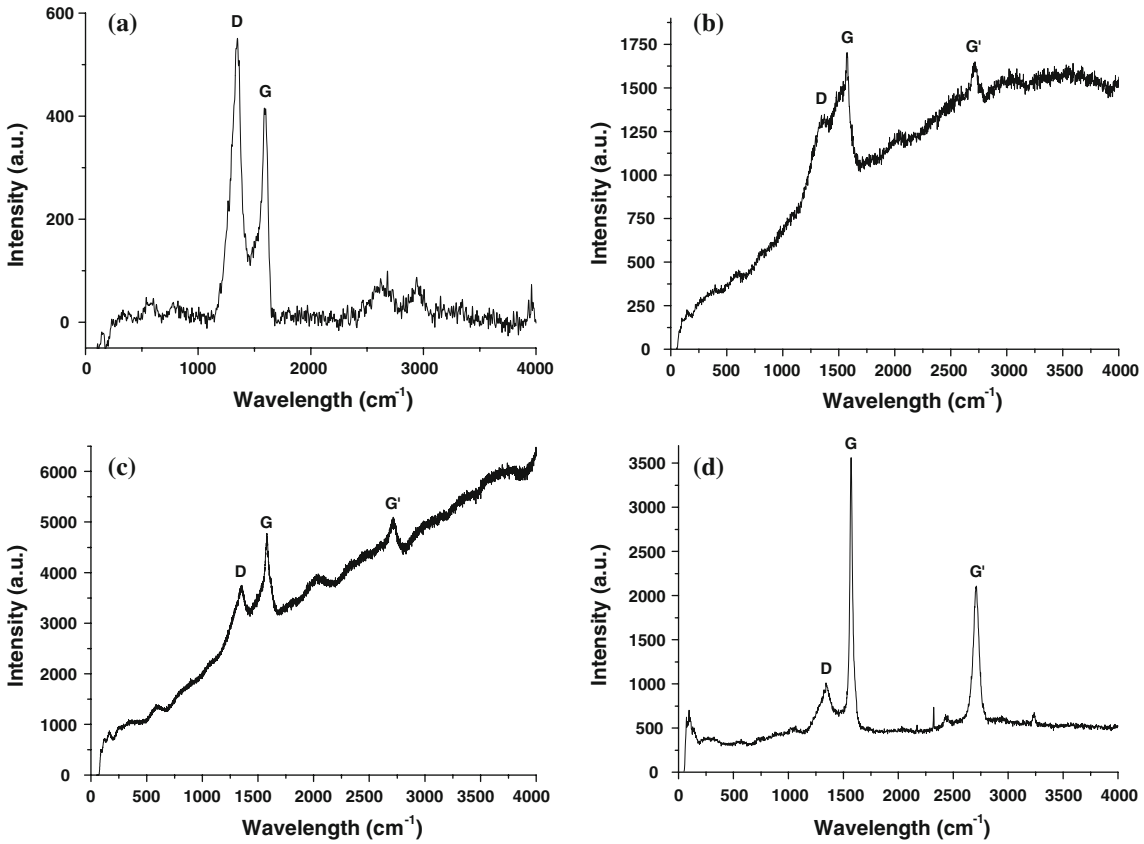

Fig. 3 Raman spectra of SiCN (**a**) and SiCN/CNT composites containing 2 vol% (**b**), 5 vol% (**c**), and 10 vol% (**d**) CNTs pyrolyzed at 1,100 °C

Table 1 Raman band positions (ω_G, ω_D), and FWHH (full width at half-height, $\Gamma_G/2$, $\Gamma_D/2$) for *G* and *D* bands and graphitization grade G_G ($G_G = I_G/(I_G + I_D)$) for as received CNTs (at r.t.), and for SiCN and SiCN/CNT materials pyrolyzed at 1,100 and 1,300 °C

Sample	Pyrolysis at 1,100 °C					Pyrolysis at 1,300 °C				
	ω_G (cm^{-1})	$\Gamma_G/2$ (cm^{-1})	ω_D (cm^{-1})	$\Gamma_D/2$ (cm^{-1})	G_G (%)	ω_G (cm^{-1})	$\Gamma_G/2$ (cm^{-1})	ω_D (cm^{-1})	$\Gamma_D/2$ (cm^{-1})	G_G (%)
SiCN	1588.0	77.3	1347.3	87.84	45.2	1592.7	95.2	1323.2	204.3	47.1
SiCN/CNT (2 vol%)	1547.3	504.3	1321.8	330.0	57.5	1563.8	86.8	1346.7	440.2	61.3
SiCN/CNT (5 vol%)	1564.8	256.1	1348.7	292.2	54.3	1564.8	45.6	1336.3	223.2	66.0
SiCN/CNT (10 vol%)	1572.1	114.7	1340.4	272.5	56.8	1534.8	252.7	1309.4	169.0	47.1
MWCNT as received	5649	296	3434	556	92.6	–	–	–	–	–

(*G* band). Confocal Raman mapping technique has been shown to be a very convenient tool for in situ characterization of phase purity of materials [28] and has been used also to assess the distribution of CNTs in composites and to investigate CNT–matrix interactions in polymer/CNT composites [29, 30]. Figure 4 illustrates the confocal Raman maps of three SiCN/CNT composites containing 2, 5, and 10 vol% CNTs pyrolyzed at 1,100 °C. Whereas in the SiCN/CNT material containing 2 vol% CNTs a fair distribution of the carbon nanotubes throughout the SiCN matrix can be evaluated (Fig. 4a), the materials with higher CNT volume fraction loadings show an enhanced quality of distribution of CNTs (Fig. 4b, c) as found also by SEM investigations.

In order to assess the percolation behavior of CNTs in the prepared polymer-derived SiCN/CNT composites, AC conductivity measurements have been performed. Thus, the critical CNT concentration (ρ_c, as vol% of CNTs) has been determined by AC conductivity measurements of composites containing CNTs loadings from 0 to 10 vol%. The AC conductivity of SiCN ceramic pyrolyzed at 1,100 °C without CNTs was found to be 10^{-9} S/cm,

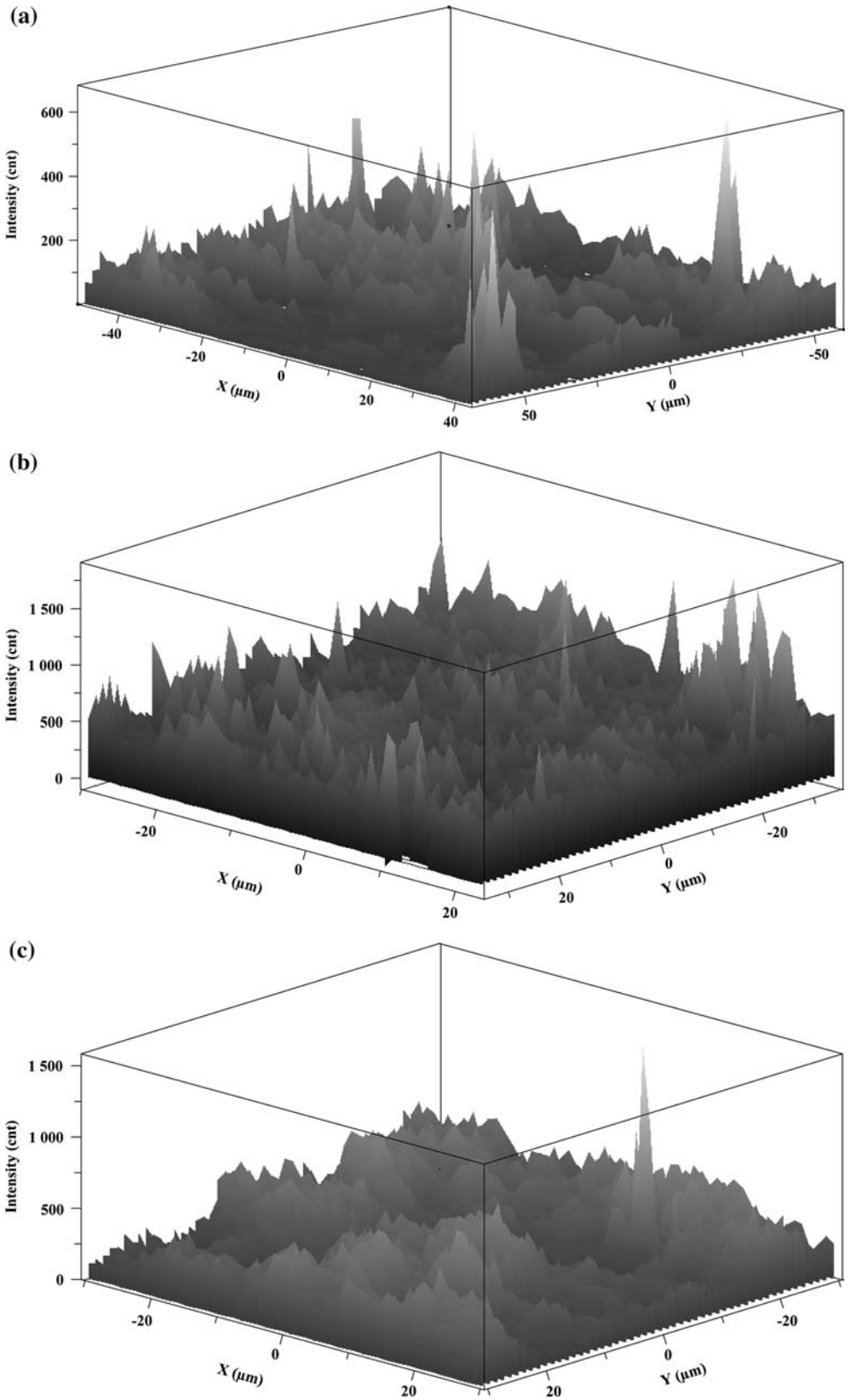

Fig. 4 3D Raman maps of *G* band (1,450–1,650 cm^{-1}) for 60 × 60 μm^2 sample surfaces of SiCN/CNT composites containing 2 vol% (**a**), 5 vol% (**b**), and 10 vol% (**c**) CNTs

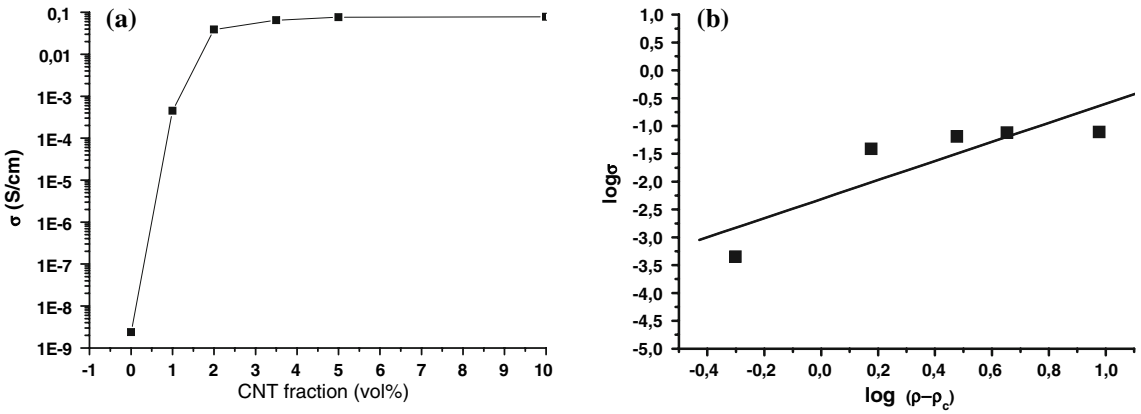

Fig. 5 **a** AC conductivities of SiCN/CNT composites pyrolyzed at 1,100 °C as function of CNT content, **b** AC conductivity as function of $\rho-\rho_c$ (double logarithmic scale) for SiCN/CNT composites containing 1, 2, 3.5, 5, and 10 vol% CNTs

revealing that the amorphous SiCN matrix is an insulator at room temperature. As shown in Fig. 5a, the conductivity increases by ca. five orders of magnitude (to 10^{-4} S/cm) if 1 vol% CNTs are added into the SiCN matrix, indicating a percolation threshold lower than 1 vol% CNTs. By further increasing the CNTs content, the AC conductivity increases moderately, and reaches 7.6×10^{-2} S/cm at 5 vol% CNTs loading, being unaltered at higher CNTs volume fractions, most probably due to agglomeration of CNTs. This is in accordance with literature known data of CNT composites, which show a dramatic increase of conductivity in a narrow range of CNT volume fraction near the percolation threshold (up to 10 orders of magnitude); subsequently, the effective conductivity can be increased further (up to three or more order of magnitude) by increasing the CNT content in the composites up to 10 vol% [31].

The percolation threshold (<1 vol%) found in the SiCN/CNT materials presented here emphasizes the good dispersion of the CNTs throughout the PDC matrix and thus supports the SEM and Raman spectroscopy results. Generally, higher percolation thresholds are found for composites containing multi-walled CNTs, e.g., 4.7 wt% in polystyrene/CNT [32], 4–6 wt% in polyamide/CNT [33, 34], or 1–2 wt% in polycarbonate/CNT composites [35].

In the last two decades, many studies have been performed in order to describe the percolation behavior in polymer/CNT composites. Thus, different models have been developed for estimating the percolation threshold in composites containing high-aspect ratio fillers. A relationship between the critical volume fraction f_c and the aspect ratio for composites in which the filler geometry is assumed to be stick-like was proposed as $(L/r) \cdot f_c - 3$ by Balberg et al. [36], with L being the length and r the radius of the fillers. Using this model for an approximation of the critical CNT concentration ρ_c in our polymer-derived SiCN/CNT composites, a higher value (3 vol%) was calculated as compared to the experimental percolation threshold which was found to be lower than 1 vol%. The mismatch between the experimental and calculated percolation threshold values can be explained by the low aspect ratio of the CNTs used for the preparation of the composites, since the Balberg model rather address composites containing high aspect ratio fillers.

Celzard [37] and Munson-McGee [38] developed an advanced percolation theory that includes the aspect ratio of particles in determining the critical volume fraction required to achieve a conducting, percolated network. The percolation threshold for rod-like fillers with aspect ratios higher than 100 was calculated to range from 0.24 to 1.35 vol% [37].

Considering the aspect ratio of 50 as in the CNTs used for our SiCN/CNT composites, a value of approximately 1.5 vol% can be calculated for ρ_c, which is still higher than that of the experimental value [39]. The fact that the experimental percolation threshold value in the case of our SiCN/CNT composites is lower than the values predicted by percolation models indicates the effectiveness of our preparation method in achieving good dispersion of CNT's throughout the matrix.

The AC conductivities of the prepared SiCN/CNT composites and the obtained percolation threshold value were used for the calculation of t, i.e., the critical exponent, which describes the dimensionality of the transport in the investigated systems. Thus, the following scaling law was used:

$$\sigma = \sigma_0(\rho - \rho_c)^t \quad (1)$$

with σ being the composite conductivity (S/cm), σ_0—an adjustable parameter, ρ—volume fraction of filler, and ρ_c—percolation threshold [40]. Figure 5b illustrates σ as a function of $\rho-\rho_c$ in the double logarithmic coordinates. Assuming a ρ_c value of 0.5 vol%, the critical exponent t was found to be 1.71.

The observed critical exponent t of the SiCN/CNT-composites indicates transport within three dimensions as for model systems of conductive particles in an insulating matrix. This is in accordance with theoretical calculations of the critical exponent t which show values from 1.1 to 1.35 for model systems with transport in two dimensions, while in the case of three dimensional transport values of 1.6 to 2 have been predicted [41].

Similar values of t were previously reported for $MgAl_2O_4$/single-walled CNT ceramic composites (t = 1.73) [42] as well as in poly(3-octylthiophene)/SWCNT (t = 2) [43] and polyimide/SWCNT polymer composites (t = 2.2) [44]. However, lower values of t have been observed for multi-walled CNT polymer composites, as in epoxy/MWCNT-based materials (t = 1.2) [45], and in polyvinyl-alcohol and poly(*m*-phenylenevinylene-*co*-2,5-dioctyloxy-phenylenevinylene) MWCNT composites (t = 1.36) [46].

The lower t values for the MWCNT composites were assumed not to reflect a dimensionality reduction in the transport and were explained by the influence of different factors such as aggregation of the CNTs during the preparation of the samples [43] or tunneling processes between nanotubes [44]. Thus, the observed value for t in the case of our polymer-derived SiCN/CNT composites emphasizes the uniform distribution of CNTs throughout the PDC matrix, as observed by means of SEM and Raman spectroscopy.

Conclusions

Polymer derived SiCN/CNT ceramic composites have been prepared by incorporation of multi-walled CNTs into a cross-linked polysilazane using a simple roll-mixing method followed by warm pressing and pyrolysis. The dispersion of MWCNTs within the polymer-derived SiCN matrix has been investigated by means of SEM and Raman spectroscopy techniques, showing a very good distribution of CNTs throughout the PDC matrix. Studies on electrical properties of the SiCN/CNT materials showed that the presence of CNTs in the insulating SiCN ceramic matrix increases its conductivity by up to seven orders of magnitude. Furthermore, an electrical percolation threshold ρ_c at values lower than 1 vol% MWCNT loading was found, thus supporting the uniform distribution of CNTs throughout the PDC matrix as demonstrated by SEM and Raman spectroscopy studies. The observed critical exponent of electrical conductivity t (1.71) indicates a transport in three dimensions and emphasizes also the good distribution of CNTs in the composite materials. Thus, using a simple roll-mixing method for incorporation of modest aspect ratio CNTs into a cross-linked polymer, SiCN/CNT ceramic composites have been obtained showing well dispersed CNTs throughout the insulating amorphous SiCN matrix. Further investigations concerning transport mechanisms as well as microstructure evolution of the synthesized SiCN/CNT composites at high-temperatures are currently in progress.

Acknowledgements AF acknowledges the support of the Alexander von Humboldt fellowship program. The authors thank Prof. Dr. Loutfi (MER Company, USA) for supplying the multi-walled CNTs used in this study and Dr. Bremes for performing the electrical conductivity measurements. RR thanks the Fonds der Chemischen Industrie for financial support.

References

1. Yakobson BI, Brabec CJ, Bernholc J (1996) Phys Rev Lett 76:2511
2. Treacy MMJ, Ebbesen TW, Gibbson JM (1996) Nature 381:678
3. Lurie O, Wagner HD (1998) J Mater Res 13:2418
4. Krishnan A, Dujardin E, Ebbesen TW, Yianilos PN, Treacy MMJ (1998) Phys Rev B 58:14013
5. Yu M, Lourie O, Dyer MJ, Moloni K, Kelly TF, Ruoff RS (2000) Science 287:637
6. Yu MF, Files BS, Arepalli S, Ruoff RS (2000) Phys Rev Lett 84:5552
7. Berber S, Kwon Y, Tomanek D (2000) Phys Rev Lett 84:4613
8. Thess A, Lee R, Nikolaev P, Dai H, Petit P, Robert J, Xu C, Lee YH, Kim SG, Rinzler AG, Colbert DT, Scuseria GE, Tomanek D, Fischer JE, Smalley RE (1996) Science 273:483
9. Hone J, Llaguno MC, Nemes NM, Johnson AT, Fischer JE, Walters DA, Casavant MJ, Schmidt J, Smalley RE (2000) Appl Phys Lett 77:666
10. Langer L, Stockman L, Heremans JP, Bayot V, Olk CH, Van Haesendonck C, Bruynseraede Y, Issi JP (1994) J Mater Res 9:927
11. Thostenson ET, Ren Z, Chou TW (2001) Comp Sci Technol 1899:61
12. Gao L, Jiang L, Sun J (2006) J Electroceram 17:51
13. An L, Xu W, Rajagopalan S, Wang C, Wang H, Fan Y, Zhang L, Jiang D, Kapat J, Chow L, Guo B, Liang J, Vaidyanathan R (2004) Adv Mater 16:2036
14. Katsuda Y, Gerstel P, Narayanan J, Bill J, Aldinger A (2006) J Eur Cer Soc 26:3399
15. Li Y, Fernandez-Recio L, Gerstel P, Srot V, van Aken PA, Kaiser G, Burghard M, Bill J (2008) Chem Mater 20:5593
16. Al-Jishi R, Dresselhaus G (1982) Phys Rev B 26:4514
17. Gruber T, Zerda TW, Gerspacher M (1994) Carbon 32:1377
18. Menargh TP, Cooney RP, Johnson RA (1984) Carbon 22:39
19. Wang Q, Allred DD, Gonzales-Hernandez J (1993) Phys Rev B 47:6119
20. Jorio A, Pimenta MA, Fantini C, Souza M, Filho Souz AG, Samsonidze GG, Dresselhaus G, Dresselhaus MS, Saito R (2004) Carbon 42:1067
21. Dresselhaus MS, Dresselhaus G, Saito R, Jorio A (2005) Phys Rep 409:47
22. Costa S, Borowiak-Palen E, Krusznynska M, Bachmatiuk A, Kalenczuk RJ (2008) Mater Sci-Poland 26:433
23. Bacsa WS, Ugarte D, Chatelain A, de Heer WA (1994) Phys Rev B 50:15473
24. Hiura H, Ebbesen TW, Tanigaki K, Takahashi H (1993) Chem Phys Lett 202:509
25. Trassl S, Motz G, Rössler E, Ziegler G (2001) J Non-Cryst Solids 293–295:261

26. Schader LS, Giannaris SC, Ajayan PM (1998) Appl Phys Lett 73:3842
27. Wang S, Liang R, Wang B, Zhang C (2008) Chem Phys Lett 457:371
28. Brillante A, Billoti I, Della Valle RG, Venuti E, Masino M, Girlando A (2005) Adv Mater 17:2549
29. Huan S, Lin W, Sato H, Yang H, Jiang J, Ozaki Y, Wu H, Shen G, Yu R (2007) J Raman Spectrosc 38:260
30. Bassil A, Puech P, Landa G, Bacsa W, Barrau S, Demont P, Lacabanne C, Perez E, Bacsa R, Flahaut E, Peigney A, Laurent C (2005) J Appl Phys 97:034303
31. Deng F, Zheng QS (2008) Appl Phys Lett 92:071902
32. Curran SA, Zhang D, Wondmagegn WT, Ellis AV, Cech J, Roth S, Caroll DL (2006) J Mater Res 21:1071
33. Meincke O, Kämpfer D, Weickmann H, Friedrich C, Vathauer M, Warth H (2004) Polymers 45:739
34. Schartel B, Pötschke P, Knoll U, Abdel-Goad M (2004) Eur Polym J 41:1061
35. Pötschke P, Fornes TD, Paul DR (2002) Polymer 43:3247
36. Balberg I, Anderson CH, Alexander S, Wagner N (1984) Phys Rev B 30:3933
37. Celzard A, McRae E, Deleuze C, Dufort M, Furdin G, Mareche JF (1996) Phys Rev B 53:6209
38. Munson-McGee SH (1991) Phys Rev B 43:3331
39. Garboczi EJ, Snyder KA, Douglas JF, Thorpe MF (1995) Phys Rev E 52:819
40. Stauffer D, Aharony A (1992) Introduction to Percolation Theory. Taylor and Francis, London
41. Weber M, Kamal MR (1997) Polym Comp 18:711
42. Rul S, Lefevre-schlick F, Capria E, Laurent C, Peigney E (2004) Acta Mater 52:1061
43. Kymakis E, Alexandou I, Amaratunga GAJ (2002) Synth Met 127:59
44. McLachlan DS, Chiteme C, Park C, Wise KE, Lowther SE, Lillehei PT (2005) J Polym Sci B: Polym Phys 43:3273
45. Sandler JKW, Kirk JE, Kinloch IA, Schaffer MSP, Windle AH (2003) Polymer 44:5893
46. Kilbride BE, Coleman JN, Fraysse J, Fournet P, Cadek M, Drury A, Hutzler S, Roth S, Blau WJ (2002) J Appl Phys 92:4024